Characterization of the Core of Polystyrene Block Poly(methyl methacrylate) Polymer Micelles by Energy Transfer

Jean Duhamel, Ahmad Yekta, Shaoru Ni, Yariv Khaykin, and Mitchell A. Winnik*

Department of Chemistry and Erindale College, University of Toronto, 80 St. George Street, Toronto, Canada M5S 1A1

*Received April 21, 1993; Revised Manuscript Received August 10, 1993**

ABSTRACT: Nonradiative direct energy transfer (DET) experiments have been employed to characterize the core of block copolymer micelles. Polystyrene-*block*-poly(methyl methacrylate) polymers (PS–PMMA) with a chromophore at the junction have been prepared by multistep living anionic polymerization. The chromophore at the junction is either a donor, phenanthrene (Phe) for polymer 1 (M_n(PS) = 11K, M_n(PMMA) = 25K), or an acceptor, anthracene (An) for polymer 2 (M_n(PS) = 11K, M_n(PMMA) = 26K). In 30/70 (w/w) dioxane–methanol mixtures, these polymers spontaneously form monodisperse block copolymer micelles. By quasi-elastic light scattering (QELS) and viscosity measurements we find that the hydrodynamic radius R_H = 19 nm and that these micelles are made of 140 polymer units. In these micelles, donors and acceptors are embedded in the core/shell interface. Two approaches are considered to study the interface where DET occurs. In the first, the interface is taken as the flat surface of a perfect sphere. In the second, the interface is assumed to be a fractal medium. These two analyses of the fluorescence decays (combined with computer simulations of the DET kinetics) give evidence that the core is swollen by the solvent and that the core/shell interface is diffuse. An apparent fractal dimension of 2.3 is recovered.

Introduction

A diblock copolymer is made of two moieties of different chemical structure, which we will refer to as B and C. In a solvent where the B-block is soluble but the C-block is not, such polymers self-assemble into micellar structures.[1] These micelles can be divided into two domains, a core made up of the insoluble B component and a shell or corona where the soluble C moieties are swollen by the solvent. Because of the intrinsic interest in self-assembling systems and because of the potential application of block copolymer micelles as dye or drug delivery vehicles,[2] these systems have been the focus of numerous investigations.[1-3] To some extent, over the past decade, this interest has been spearheaded by the tremendous advances in the theory of block copolymer micelle structure and dynamics.[4-9]

A variety of different techniques have been employed to examine block copolymer association. The most reliable results on micelle structure have come from light scattering and X-ray scattering studies involving the index matching technique, through the choice of solvents isorefractive to one or the other copolymer block. All these techniques aim at obtaining relevant parameters for these systems, such as the hydrodynamic radius (R_H) or the aggregation number (N_{agg}), as well as the core radius and the shell thickness. According to theory, these parameters should follow scaling laws with copolymer chain length and individual block length. Most of the parameters obtained by these techniques are averaged values. Measuring a hydrodynamic radius gives an estimate of the micelle radius, but it is only one measure of the real structure.

In a study aimed at determining sizes, the best means available to an experimentalist is to use a ruler. In the present study, we wish to employ a spectroscopic ruler.[10] Our approach is based on direct non-radiative energy transfer (DET). We have synthesized PS–PMMA block copolymers that contain at the B/C junction a phenanthrene group or an anthracene group chosen to act as donor and acceptor, respectively.[11] Due to their position on the block copolymer backbone, the chromophores are expected to locate themselves at the block copolymer micelle core/shell interface.

DET occurring between a donor molecule (D) and an acceptor molecule (A) is well described by Scheme I. After absorption of a photon, an excited donor molecule D* can relax either by fluorescence with a rate constant $1/\tau_D$, where τ_D is the unquenched donor lifetime, or by DET with a rate constant $k(r)$. $k(r)$ depends on the distance r between the centers of the transition moments of the donor and acceptor species. For DET by the dipole coupling (Förster) mechanism, $k(r)$ is given by

$$k(r) = \left(\frac{R_0}{r}\right)^6 \frac{1}{\tau_D} \tag{1}$$

Here, R_0 is the critical Förster radius which is determined by the donor-acceptor spectral overlap integral. It establishes the length scale for DET.

Due to the radial dependence of the DET rate constant, this technique is routinely used as a spectroscopic ruler for the study of chemical and biological microsystems.[10,12] In the present experiments, DET is applied to PS–PMMA copolymer micelles, and information about the core structure is obtained. Micelles formed from PS–PMMA block copolymers in selective solvents were studied extensively by light scattering more than a decade ago[13a,b] and more recently by neutron scattering.[13c]

Theory

When donor and acceptor molecules are introduced into a solid matrix, the acceptor molecules occupy sites surrounding the donor molecules with a site density function $\rho'(r)$. For an acceptor-site-occupancy probability p, the survival probability of the excited donor $\phi(t)$ is given by

$$\phi(t) = \exp\left(-\frac{t}{\tau_D}\right) \exp\{-p\int \rho'(r)[1 - \exp(-k(r)t)]\, dr\} \tag{2}$$

In this expression, the integral is calculated over the total volume in which DET occurs.

* Abstract published in *Advance ACS Abstracts*, October 1, 1993.

0024-9297/93/2226-6255$04.00/0

Scheme I

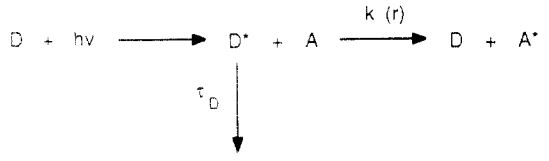

Recently, Klafter and Blumen (KB) proposed a generalization of the Förster equation for the survival probability of an excited donor.[14] When donor and acceptor molecules are distributed in an exact fractal medium, KB show that $\phi(t)$ can be described by eq 3

$$\phi(t) = \exp\left(-\frac{t}{\tau_D} - c\left(\frac{t}{\tau_D}\right)^{\bar{d}/6}\right) \tag{3}$$

where $\bar{d}$ is the fractal dimension of the medium and c is a time-independent factor that is proportional to the acceptor concentration. Research groups interested in the study of chemical or biological microstructures have pointed out that eq 3 could be also applied to nonfractal restricted geometries.[15] In this case, $\bar{d}$ is called the "effective" or "apparent" dimension. Thus, eq 3 can in principle be applied to any system where DET occurs. The values of c and $\bar{d}$ recovered from eq 3 characterize the system under study.

We are interested in probing the core/shell interface of block copolymer micelles. This boundary is expected to be either (1) sharp in the case of a solvent-free micelle core or (2) loose in the case of a micelle core swollen by solvent. In case 1, donor and acceptor molecules can be thought of as incorporated into the surface of a sphere. On the other hand, in case 2, donor and acceptor molecules are distributed at the core/shell interface in a spherical shell of finite thickness. There, the chromophores probe a volume instead of a surface, and eq 3 should retrieve an apparent dimension between 2 and 3. If donor and acceptor molecules in case 1 are located on a sufficiently small sphere, it is also possible that DET occurs across the sphere's diameter. This may introduce additional finite geometry constraints to the energy transfer kinetics.

Because of this, the use of eq 3 alone is not enough to distinguish between cases 1 and 2, and extra knowledge is required about the system's geometry. One useful approach to obtaining additional information is through simulation of fluorescence decays for DET in known geometries and then fitting them with eq 3. In so doing, it is possible to examine the behavior of eq 3 in controlled situations. Simulations have provided good insight into the kinetics of DET occurring on the surface of infinitely long cylinders.[16]

Turning to eq 2, we consider an ensemble of identical restricted volumes V of undefined dimensionality, each with on average $\langle n \rangle$ randomly distributed acceptors. The definition of p yields

$$p = \frac{\langle n \rangle}{\int_V \rho'(r)\, dr} \tag{4}$$

We define $\rho(r)\, dr$ as the probability of finding a given donor–acceptor pair, separated by a distance r, between r and $r + dr$.

$$\rho(r)\, dr = \frac{\rho'(r)\, dr}{\int_V \rho'(r)\, dr} \tag{5}$$

Using these definitions, eq 2 can be rewritten as

$$\phi(t) = \exp\left(-\frac{t}{\tau_D}\right) \exp\{-\langle n \rangle \int_V \rho(r)[1 - \exp(-k(r)t)]\, dr\} \tag{6}$$

Note that in the case where $k(r)$ is independent of r (i.e., $k(r)$ = constant), we recover the classical expression for diffusional quenching in surfactant micelles.[17] This result is important because it makes explicit the connection between classical micelles as systems of restricted geometry and the KB equation.

The utility of eq 6 depends on our ability to calculate the integral

$$I(t) = \int_V \rho(r)[1 - \exp(-k(r)t)]\, dr \tag{7}$$

and integrating eq 7 requires knowledge of $\rho(r)$. In the case of DET occurring on the surface of a sphere of radius R, $\rho(r)$ has an exact expression given by eq 8.[18]

$$\rho(x) = x/2 \quad \text{with } x = r/R \tag{8}$$

Because of van der Waals interactions, the donor and acceptor molecules cannot approach each other any closer than a distance b which depends on their average van der Waals size. $I(t)$ is then equal to

$$I(t) = \int_{b/R}^{2} \rho''(x)\left[1 - \exp\left(-\left(\frac{R_0}{R}\right)^6 \frac{t}{\tau_D} \frac{1}{x^6}\right)\right] dx \tag{9}$$

where

$$\rho''(x) = \frac{\rho(x)}{\int_{b/R}^{2} \rho(x)\, dx} \tag{10}$$

We can now calculate $I(t)$. Introducing its value into eq 6, we have access to the survival probability $\phi(t)$.

Equation 6 is exact. Nevertheless, it has been shown that for times $(b/R_0)^6\tau_D \ll t \ll 2(R/R_0)^6\tau_D$, it can be reduced to[18]

$$\phi(t) = \exp\left(-\frac{t}{\tau_D} - \langle n \rangle \frac{\Gamma\left(\frac{2}{3}\right)}{4}\left(\frac{R_0}{R}\right)^2\left(\frac{t}{\tau_D}\right)^{1/3}\right) \tag{11}$$

with

$$\Gamma\left(\frac{2}{3}\right)/4 = 0.339 \tag{12}$$

Under such conditions, a fractal analysis of donor fluorescence decays using eq 3 should lead to a dimension $\bar{d}$ equal to 2. A plot of c versus $\langle n \rangle$ should be linear with a slope equal to $0.339(R_0/R)^2$.

Numerical integration of $I(t)$, using eq 7, was performed for three different values of R ($R = 2R_0$, $5R_0$, $10R_0$), assuming values of $R_0 = 25$ Å, $b = 10$ Å, and $\tau_D = 50$ ns. These values are characteristic of the phenanthrene/anthracene pair. Subsequently, $I(t)$ was inserted into eq 6, and $\phi(t)$ was evaluated for different values of $\langle n \rangle$. To fulfill the experimental requirements of the single-photon-counting technique, eq 6 was convoluted with an experimental lamp function, and Poisson noise was added to the fluorescence decays. Fluorescence decays were generated with 20 000 counts, at the maximum peak channel, over 256 channels with a time per channel of 1.04 ns. These are the typical experimental conditions we employ when working with phenanthrene derivatives. They satisfy the conditions for application of eq 11. Fractal analysis was carried out on the simulated fluorescence decays to

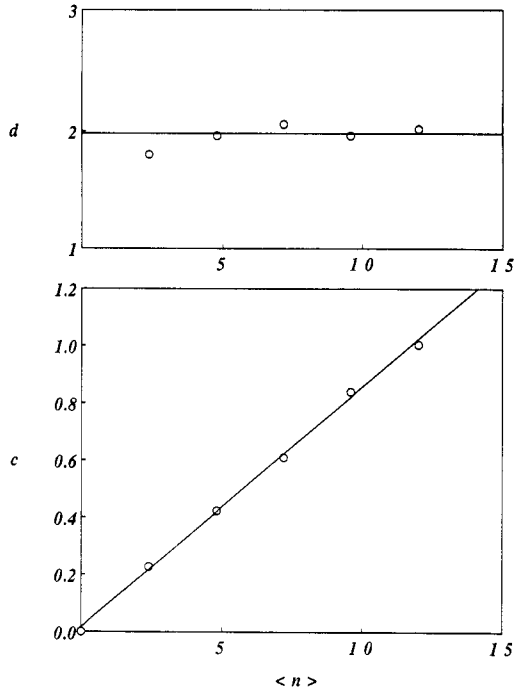

Figure 1. Analysis of simulated decay profiles for energy transfer on the surface of a small sphere: plot of c and $\bar{d}$ versus $\langle n \rangle$. These simulated fluorescence decays were generated with R_0 = 25 Å, b = 10 Å, and $R = 2R_0$.

Table I. Parameters[a] Obtained from Analysis of Simulated Fluorescence Decay Curves for DET between Donor–Acceptor Pairs on the Surface of a Sphere of Radius R (R_0 = 25 Å, b = 10 Å)

R/R_0	$\langle \bar{d} \rangle$[b]	m[c]	$m(R/R_0)^2$
2	1.96	8.40×10^{-2}	0.336
5	2.01	1.34×10^{-2}	0.335
10	1.97	3.46×10^{-3}	0.346

[a] Values shown are the average of five independent simulations of fluorescence decays for three choices of R/R_0. Individual values exhibited a variation of 2% about the average. [b] The averaged effective dimensionality obtained by fitting the data to eq 3. [c] Slope of the plot of c vs $\langle n \rangle$.

establish the reliability of this method for the study of our system.

Fits of fluorescence decays by eq 3 yield values of c and $\bar{d}$, which were plotted against $\langle n \rangle$. For the three spherical radii investigated, c was linear in $\langle n \rangle$, while $\bar{d}$ was constant and close to 2. Figure 1 shows one such typical plot for $R = 2R_0$. In all three cases, the slopes (m) of the plots are in agreement with eq 11 within ±2%. The results from the fractal analysis of the simulated decay curves are summarized in Table I.

In summary, fluorescence decays were simulated assuming DET to occur between donors and acceptors located on the surface of spheres with radii ranging from $2R_0$ to $10R_0$. This study shows that the fractal analysis complies with eq 11 for the sphere sizes considered here. The apparent dimension is equal to 2, and plots of c versus $\langle n \rangle$ are linear with a slope of $0.339(R_0/R)^2$. This behavior holds for spheres with radii as small as $2R_0$. It is interesting to note that even here, the DET fractal analysis is not affected by the small radius of curvature.

Experimental Section

Block Copolymer. For the purpose of our study, three PS–PMMA block copolymers were available (cf. Table II). Their synthesis has been described elsewhere.[11] The polymers were purified by repeated precipitation into methanol from CH_2Cl_2 solution and analyzed by gel permeation chromatography (GPC) using tandem refractive index and UV or fluorescence detectors. These samples containing up to 2 wt % polystyrene homopolymer as an impurity. Low molecular weight UV-absorbing impurities were always less than 0.01%. Since PMMA and PS have very similar calibration curves for GPC in tetrahydrofuran, M_n and M_w/M_n values for both the PS block and the entire block copolymer could be determined by GPC. The polymer composition was determined by ^{1}H NMR. The chromophore content was determined by UV spectroscopy from knowledge of the polymer M_n values, using 1-(9-phenanthryl)-1-phenylethane and 9-methylanthracene as model compounds.

Table II. Characteristics of the PS–PMMA Diblock Copolymer Samples

sample name	structure	M_n(PS/PMMA)	M_w/M_n
polymer 1	PS–Phe–PMMA	11K/25K[a]	1.12
polymer 2	PS–An–PMMA	11K/26K	1.15
polymer 3	PS–PMMA	11K/27K	1.13

[a] M_n(PS) = 11000; M_n(PMMA) = 25000.

Sample Preparation. The solvent composition at which PS–PMMA block copolymer micelles are formed is very specific. Both PS and PMMA are soluble in dioxane. PS is insoluble in methanol. For the block copolymer sample under investigation, micelles are formed in a 30/70 mass percent mixture of dioxane–methanol. Higher methanol content induces aggregation. Lower methanol content does not allow micelle formation. Temperature and polymer concentration are two other important parameters for the stability of the micellar solutions. For example, at 22 °C, a 4 g/L polymer solution flocculates. To prevent micellar aggregation, all experiments were performed at 30 °C and at polymer concentrations below 8 g/L.

Concentrated polymer stock solutions were prepared in dioxane (typically 40 g/L). Under vigorous magnetic stirring, a known volume of stock solution was added rapidly to the volume of warm methanol that is required to ensure a 30/70 (wt %) dioxane–methanol mixture. When methanol and the dioxane stock solution are mixed, the solution initially is milky, but clarifies after vigorous stirring for a few seconds. The resulting solution exhibits a slight purple tinge due to light scattering from block copolymer micelles.

Solutions used for fluorescence measurements were degassed by nitrogen bubbling. For fluorescence measurements, mixtures of polymers 1 and 2 were used. The total polymer concentration was kept constant (2 g/L) and the ratio of polymer 1 to polymer 2 was changed, thus changing the amount of acceptors per micelle.

All solutions were prepared with spectrograde quality solvents. Spectrograde 1,4-dioxane, methanol, and cyclohexane were from Caledon.

QELS Measurements. QELS measurements were carried out on a Brookhaven particle sizer Model BI-90. These measurements performed on our polymer solutions at 30 °C show that the block copolymer micelles are monodisperse in size (Figure 2). QELS yields the diffusion coefficient D of the particle in solution. For hard spheres, the radius of the sphere σ is related to D by eq 13

$$D = \frac{k_B T}{6\pi\eta\sigma} \tag{13}$$

where k_B is the Boltzmann constant, T is the absolute temperature, and η is the viscosity of the solvent.

Block copolymer micelles are not hard spheres but rather loose structures due to the swelling of the corona by solvent. However, the solvent molecules are assumed to move almost in unison with the whole structure as though the solvent were bound to the polymer. This leads to the concept of an equivalent hydrodynamic sphere with a corresponding hydrodynamic radius R_H. By considering block copolymer micelles as equivalent hydrodynamic spheres, the application of eq 13 yields hydrodynamic radii of 19 nm for polymer 1, 20 nm for polymer 2, and 18.5 nm for polymer 3.

Viscosity Measurements. To obtain the aggregation number N_{agg} of the micelles, viscosity measurements were carried out on

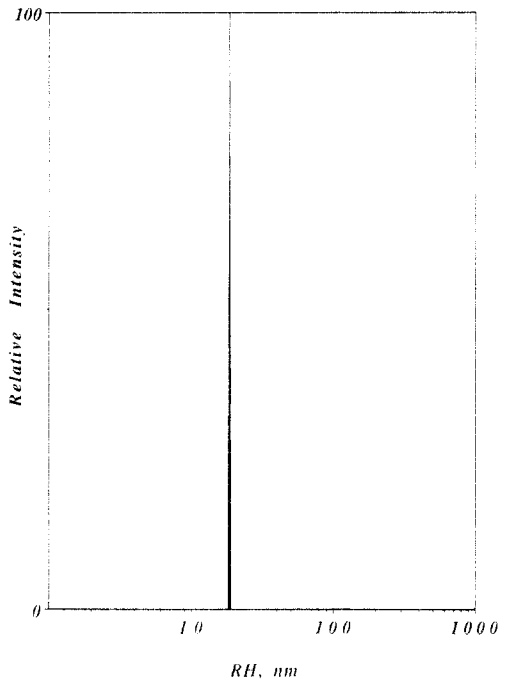

Figure 2. Size distribution of block copolymer micelles as recovered by QELS. R_H is the hydrodynamic radius. $\langle R_H \rangle$ = 18.5 nm; dimensionless polydispersity σ_G = 0.020 ± 0.005.

the chromophore-free polymer 3. A Ubbelohde viscometer in a constant-temperature bath was employed. Combining the Einstein and Stokes laws for spherical particles of radius R_H, we obtain the following relationship:

$$[\eta] = \frac{10\pi}{3}\frac{NR_H^3}{N_{agg}M_n} \tag{14}$$

where N is the Avogadro number, $[\eta]$ is the intrinsic viscosity of the block copolymer micelles, and M_n is the molecular weight of one copolymer unit forming the micelle. In this work, the unlabeled polymer has an M_n value of 38 000. Viscosity measurements performed on five copolymer concentrations give an intrinsic viscosity of 75 mL/g. We find an aggregation number of 140 polymer units per micelle. This value is in good agreement with other results on block copolymer micelles.[1,19]

UV-Vis Absorption and Dynamic and Static Fluorescence Measurements. UV measurements were carried out on a Perkin-Elmer Lambda 2 UV-vis double-beam spectrometer. Fluorescence spectra were obtained on a SPEX Fluorolog 112 spectrometer. Decay curves were obtained by the time-correlated single-photon-counting (SPC) technique. The excitation source was a coaxial flash lamp (Edinburgh Instruments Model 199F). The excitation wavelength was selected by a Jobin-Yvon Model H-20 monochromator, and that of the fluorescence by a SPEX Minimate Model 1760 monochromator. The analysis of the excited phenanthrene decay curves was performed by the MIMIC deconvolution method. Reference decay curves of degassed solutions of 2,5-diphenyloxazole (PPO) in cyclohexane (τ = 1.33 ns) were used for the analysis of phenanthrene decay curves. For SPC measurements, the excitation wavelength was 300 nm and the phenanthrene fluorescence was observed at 349 nm. For steady-state measurements, the excitation wavelength was 300 nm, except in the study for the R_0 determination, where it was fixed at 293.3 nm. For UV absorption or static fluorescence measurements, the spectra from solutions of labeled block copolymer micelles were corrected for light scattering by subtracting the spectra obtained with solutions of unlabeled block copolymer micelles of identical concentration.

***R_0* Determination.** The quantum yield of phenanthrene-labeled block copolymer micelles (BCM-Phe), ϕ_{mic}, was determined by comparison with the quantum yield of phenanthrene in cyclohexane (ϕ_{cx} = 0.13).[20] Optically dilute solutions (Abs-

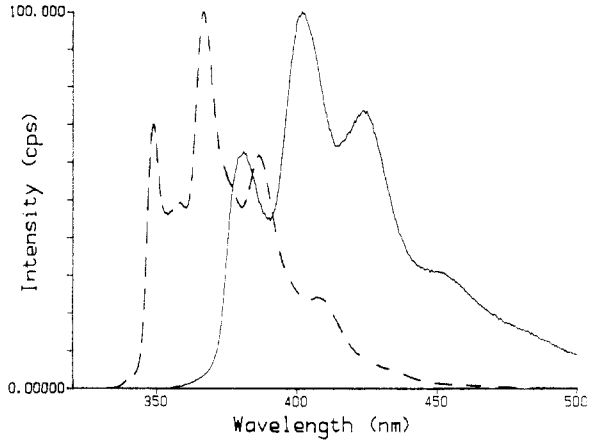

Figure 3. (- - -) Phenanthrene emission from block copolymer micelles made of polymer 1 (λ_{ex} = 300 nm); (—) anthracene emission from block copolymer micelles made of polymer 2 (λ_{ex} = 358 nm).

(λ_{ex}) < 0.1) were prepared so that eq 15 applies.[21]

$$\phi_{mic} = \phi_{cx}\left(\frac{\mathrm{Abs}_{cx}(\lambda_{ex})}{\mathrm{Abs}_{mic}(\lambda_{ex})}\right)\left(\frac{n_{mic}^2}{n_{cx}^2}\right)\left(\frac{\int_0^\infty F_{mic}(\lambda)\,d\lambda}{\int_0^\infty F_{cx}(\lambda)\,d\lambda}\right) \tag{15}$$

Abs(λ_{ex}) is the solution absorbance at the excitation wavelength λ_{ex} and n is the refractive index of the solvent. The indices cx and mic refer to cyclohexane and the 30/70 mass percent dioxane–methanol mixture, respectively. For cyclohexane, n_{cx} = 1.426 and for a 30/70 mass percent dioxane–methanol mixture, n_{mic} = 1.355. $\int F(\lambda)\,d\lambda$ is the integrated area under the fluorescence spectrum. For both solutions, the excitation wavelength was fixed at 293.3 nm. This wavelength corresponds to an absorption maximum for phenanthrene in cyclohexane and to an absorption minimum for BCM-Phe. The 293.3-nm absorption maximum of Phe in cyclohexane is shifted to 300 nm for BCM-Phe. A quantum yield of 0.23 is obtained for BCM-Phe.

R_0 is the critical Förster radius and is determined by the donor–acceptor spectral overlap integral following eq 16.

$$R_0^6 = \frac{9000\ln(10)\,(2/3)\phi_D}{128\pi^5 n^4 N}\frac{\int_0^\infty F_D(\nu)\,\epsilon_A(\nu)\frac{d\nu}{\nu_4}}{\int_0^\infty F_D(\nu)\,d\nu} \tag{16}$$

Here, $\epsilon(\nu)$ is the acceptor molar extinction coefficient and ν is the wavenumber. The indices A and D refer to acceptor (anthracene) and donor (phenanthrene), respectively. For the donor–acceptor pair phenathrene/anthracene in block copolymers, R_0 = 22 Å. This value compares well with previous results.[22]

Results and Discussion

Solutions of phenanthrene in cyclohexane exhibit well-resolved fluorescence spectra where most of the fluorescence is emitted between 330 and 450 nm. Micellar solutions of polymer 1 behave in a similar manner, as shown in Figure 3. When SPC measurements are carried out on such solutions, single-exponential decays are recovered with lifetimes of 45.5 ns. This is the unquenched donor lifetime τ_D. When excited at 358 nm, micellar solutions of polymer 2 exhibit a typical anthracene fluorescence spectrum. When micelles are made of a mixture of polymers 1 and 2 and the solution is excited at 300 nm, the fluorescence spectrum is a superposition of phenanthrene and anthracene emissions (Figure 4). This emission is essentially due to anthracene molecules that are excited by DET from previously excited phenanthrene molecules. Fluorescence decays of such solutions are more complicated, as shown in Figure 5. Analysis of this profile (cf. Figure 6) gives information on the process of energy transfer.

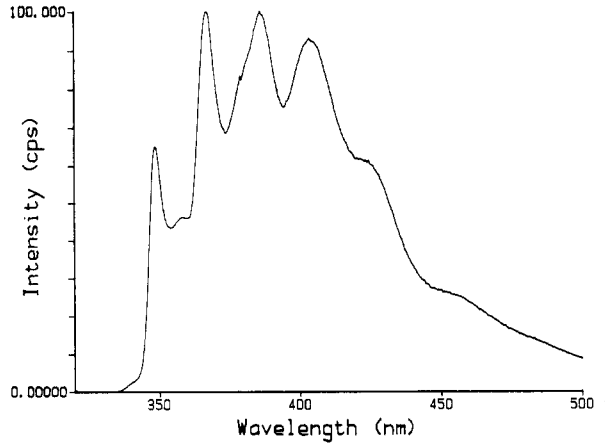

Figure 4. Fluorescence spectrum of a 1:1 mixture of polymers 1 and 2 (λ_{ex} = 300 nm) in 30/70 (w/w) dioxane–methanol at 2.0 g/L.

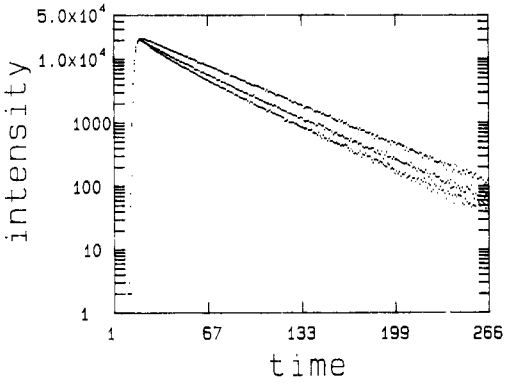

Figure 5. Donor fluorescence decay profiles for different donor–acceptor ratios. From top to bottom, 100:0 (polymer 1 only), 60:40, 35:66 (concentration 2.0 g/L in 30/70 (w/w) dioxane–methanol.

Six solutions of block copolymer were prepared, keeping the total polymer mass content constant (2 g/L) but varying the 1:2 ratio. In this way we could vary the acceptor concentration within each micelle without affecting the size of the micelle or its aggregation number. In terms of our data analysis, we are able to vary $\langle n \rangle$ without otherwise perturbing the system.

In a first approach, we assume the core of the block copolymer micelles to have a sharp core/shell interface and analyze the fluorescence decays with eq 3, fixing the apparent dimension to 2. This is equivalent to fitting the fluorescence decays with eq 11. The micellar core is taken to be a sphere with the donors and acceptors in its surface. The fits of fluorescence decays were good ($\chi^2 < 1.2$; residuals and autocorrelation function of the residuals randomly distributed around zero), and the plot of c versus $\langle n \rangle$ is linear (Figure 7). The recovery of a linear plot is a key feature when dealing with DET experiments, as the c factor is required to be proportional to the acceptor concentration. Analysis of the slope in Figure 7 with eq 11 gives a ratio R/R_0 of 6.3. From the theoretical considerations of the previous section, we know that this value lies in the range where eq 11 applies. Since R_0 = 22 Å, we calculate an R value of 14 nm.

In terms of our model, this value pertains to a key structural parameter of the micelle; its core radius. If the core of the micelle were free of solvent, we could estimate the core radius from knowledge of N_{agg} and the density of PS. This analysis yields a core radius of 8.4 nm, which is smaller than the 14-nm value calculated from analysis of the DET measurements. It is not surprising that the dioxane in the solvent medium would swell the micelle

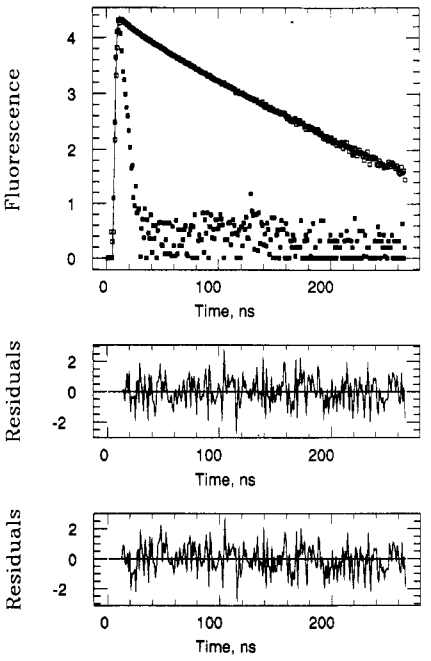

Figure 6. Comparative analysis of the lowermost decay profile in Figure 5. Here we show that we obtain fits of comparable quality to the expressions (cf. eqs 3 and 11) $\phi(t) = \exp[-t/45.5 - 0.648t^{0.398}]$ (χ^2 = 0.97, upper plot of weighted residuals) and $\phi(t) = \exp[-t/45.5 - 0.768t^{0.333}]$ (χ^2 = 1.04, lower plot of weighted residuals). In the former case, the exponent of t/τ_D is fitted to its "best" value, whereas in the second case, it is fixed at 1/3.

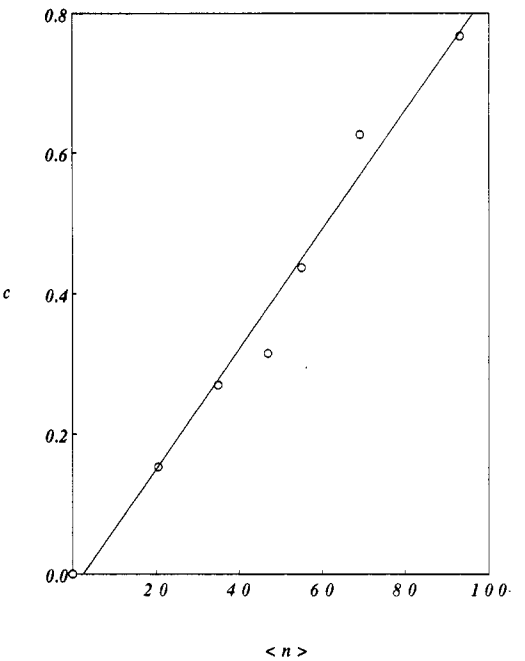

Figure 7. Plot of experimental values of c versus $\langle n \rangle$. The data are analyzed with eq 11 in which DET is assumed to occur on the surface of a sphere.

core. If these radii were taken at face value, swelling of the core by selective solvent absorption would increase its volume by a factor of 4.6, a result which is in itself not unreasonable.[13a]

Extensive swelling of the micelle core would likely also be accompanied by a broadening of the interface between the core and the surrounding corona. In this case, the donor and acceptor groups would no longer be restricted to the surface of a sphere. Rather, they would be confined within a spherical shell of finite thickness. This is the type of restricted geometry situation where eq 3 is expected to provide useful insights.

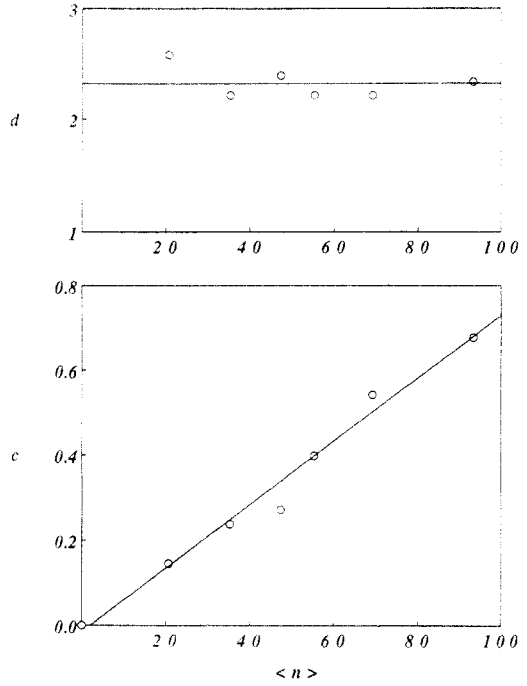

Figure 8. Plot of experimental values of c and $\bar{d}$ versus $\langle n \rangle$. The data are analyzed with eq 3 in which DET is assumed to occur in a fractal medium.

In a second approach, we carried out a fractal analysis of our fluorescence decays. Decays were fitted using eq 3, but the apparent dimension was not fixed (cf. Figure 6). Here again, the fits were good. The plot of c versus $\langle n \rangle$ is linear and a constant apparent dimension is recovered (Figure 8). The recovery of a linear plot of c vs $\langle n \rangle$ is fundamental to establishing the validity of this type of data analysis, since c is essentially equal to the mean acceptor concentration within a sphere of radius R_0 around each donor. Interpretation of the $\bar{d}$ behavior is more problematic, particularly since restricted-geometry examples in which both donors and acceptors are distributed within a volume have not been treated theoretically. One anticipates that if the restricted geometry leads to a crossover in the DET kinetics, some evolution of $\bar{d}$ with $\langle n \rangle$ should occur. Here one might expect $\bar{d} = 3$ for closely spaced pairs, which undergo rapid DET, evolving into $\bar{d} = 2$ for surviving pairs separated by larger distances. In terms of fitting data to eq 3, each experiment would give some effective $\bar{d}$ taking a value between 2 and 3, and these experiments at larger $\langle n \rangle$ should be more heavily dominated by closely spaced donor–acceptor pairs.

Alternatively, a nonrandom distribution of donor–acceptor pairs in the interface, reflecting perhaps the polymer segment density profile in the interface, could be responsible for determining the magnitude of $\bar{d}$. Under these circumstances, $\bar{d}$ would be independent of $\langle n \rangle$ and reflect some underlying structure in the pair distribution. From our data analysis, we obtain an average apparent dimensionality of 2.3. This indicates that the donors and acceptors probe a space whose dimensionality is larger than 2. The scatter in individual $\bar{d}$ values does not allow us to resolve a crossover versus a constant value of $\bar{d}$ in the system. Our results are, however, entirely consistent with a diffuse interface at the core–corona boundary.

Conclusion

DET has been employed as a spectroscopic ruler to investigate the core–corona interface of block copolymer micelles. Experiments were carried out on mixtures of three otherwise identical PS–PMMA block copolymer samples which differ only in the substituent attached to the block junction. These polymers form spherical micelles (R_H = 18.5 nm) in a solvent containing dioxane and methanol. Careful analysis of donor fluorescence decay profiles yielded information about the core size and the structure of the core/shell interface. Two limiting models both indicate that the interface between the core and the corona is diffuse, presumably a consequence of swelling of the PS core by dioxane in the solvent. A two-dimensional DET model gives the result that R_{core} = 14 nm, whereas a fractal DET model characterizes the interface as having an effective apparent dimensionality equal to 2.3.

Acknowledgment. The authors thank NSERC Canada and the Ontario Centre for Materials Research for their support of this research.

References and Notes

(1) (a) Tuzar, Z.; Kratochvil, P. *Adv. Colloid Interface Sci.* **1976**, *6*, 201; *Surf. Colloid Sci.* **1993**, *15*, 1. (b) Riess, G.; Badahur, P.; Hurtrez, G. *Encyclopedia of Polymer Science and Technology*; Wiley: New York, 1985; Vol. 2, p 324.
(2) Emmelius, M.; Hoerpel, G.; Ringsdorf, H.; Schmidt, B. In *Polymer Science and Technology*; Chiellini, E., Giusti, P., Migliaresi, C., Nicolais, L., Eds.; Plenum: New York, 1986; Vol. 34, p 313.
(3) Munch, M. R.; Gast, A. P. *Macromolecules* **1988**, *21*, 1360. Vagberg, L. J. M.; Cogan, K. A.; Gast, A. P. *Macromolecules* **1991**, *24*, 1670.
(4) Alexander, S. *J. Phys. (Paris)* **1977**, *38*, 977, 983.
(5) de Gennes, P.-G. In *Solid State Physics*; Liebert, J., Ed.; Academic: New York, 1978; Supplement 14, p 1.
(6) Noolandi, J.; Hong, M. H. *Macromolecules* **1983**, *16*, 1443.
(7) Leibler, L.; Orland, H.; Wheeler, J. C. *J. Chem. Phys.* **1983**, *79*, 3550.
(8) Nagarajan, R.; Ganesh, K. *J. Chem. Phys.* **1989**, *90*, 5843.
(9) Halperin, A. *Macromolecules* **1987**, *20*, 2934.
(10) Stryer, L. *Annu. Rev. Biochem.* **1978**, *40*, 819.
(11) Ni, S.; Juhué, D.; Moselhy, J.; Wang, Y.; Winnik, M. A. *Macromolecules* **1992**, *25*, 496.
(12) Drake, J. M.; Klafter, J.; Levitz, P. *Science* **1991**, *251*, 1574.
(13) (a) Kotaka, T.; Tanaka, T.; Hattori, M.; Inagaki, H. *Macromolecules* **1978**, *11*, 138. (b) Kotaka, T.; Tanaka, T.; Inagaki, H. *Polym. J.* **1972**, *3*, 327, 338. (c) Gast, A., personal communication.
(14) Klafter, J.; Blumen, A. *J. Chem. Phys.* **1984**, *80*, 875.
(15) (a) Yang, C. L.; Evesque, P.; El-Sayed, M. A. *J. Phys. Chem.* **1985**, *89*, 3442. (b) Yang, C. L.; El-Sayed, M. A.; Suib, S. L. *J. Phys. Chem.* **1987**, *91*, 3442.
(16) Levitz, P.; Drake, J. M.; Klafter, J. *Chem. Phys. Lett.* **1988**, *148*, 557.
(17) Yekta, A.; Aikawa, M.; Turro, N. J. *Chem. Phys. Lett.* **1979**, *63*, 543.
(18) Levitz, P.; Drake, J. M.; Klafter, J. *J. Chem. Phys.* **1988**, *89*, 5224.
(19) Xu, R.; Winnik, M. A.; Riess, G.; Chu, B.; Croucher, M. D. *Macromolecules* **1992**, *25*, 644.
(20) Berlman, I. B. *Handbook of Fluorescence Spectra of Aromatic Molecules*, 2nd ed.; Academic: New York, 1971.
(21) Demas, J. N.; Crosby, G. A. *J. Phys. Chem.* **1971**, *75*, 991.
(22) Wang, Y.; Zhao, C.-L.; Winnik, M. A. *J. Chem. Phys.* **1991**, *95*, 2143.